Acta Sci. Pol.
Formatio Circumiectus 25 (1) 2026, 29–43
ENVIRONMENTAL PROCESSES
www.acta.urk.edu.pl ISSN 1644-0765 DOI: http://dx.doi.org/10.15576/ASP.FC/217874
ORIGINAL PAPER Accepted: 06.02.2026

APPLYING 2D MIKE+ HYDRAULIC MODEL FOR FLUVIAL AND PLUVIAL FLOOD INUNDATION MODELING: EVIDENCE FROM A CASE STUDY IN SLOVAKIA

Matej Vojtek[1, 2]✉ 0000-0001-9369-3173, Jana Vojteková[1] 0000-0002-8904-9673

[1] Department of Geography, Geoinformatics and Regional Development, Faculty of Natural Sciences and Informatics, Constantine the Philosopher University in Nitra, Nitra, Slovakia
[2] Institute of Geography, Slovak Academy of Sciences, Bratislava, Slovakia

ABSTRACT

Aim of the study
The study aims to simulate the extent and depth of fluvial and pluvial flooding under different scenarios using the 2D hydraulic MIKE+ model in combination with geographic information systems (GIS).

Material and methods
As for the fluvial floods, we used steady-state flow conditions for three flood scenarios (Q_{10}, Q_{100}, and Q_{1000}). The modeled flood maps were compared to official flood maps created under the second cycle of EU Floods Directive (2007). Regarding the pluvial flooding, we used the rain-on-grid method, where the rainfall input was set to three constant intensities (20, 40, and 60 mm/hour) under two scenarios: fully saturated soils and infiltration losses. Study area was a 3.68 km section of the Teplica River in western Slovakia.

Results and conclusions
Based on the results, the flood extent difference against the official flood maps was 0.009, 0.075, and 0.123 km^2 for Q_{10}, Q_{100}, and Q_{1000}, respectively. In case of 20, 40, and 60 mm/hour rainfall scenarios and fully saturated soils, 13.5, 22.1, and 29.2% of the domain, respectively, had flow depths between 0.005–0.1 m, while 2.0, 4.2, and 6.1% of the domain had flow depths above 0.1 m. In case of 20, 40, and 60 mm/hour rainfall scenarios with infiltration losses, 6.0, 14.6, and 22.7% of the domain, respectively, had flow depths between 0.005–0.1 m, while 0.4, 2.5, and 4.5% of the domain had flow depths above 0.1 m. When the infiltration rates of land cover classes are applied, pluvial flood extent decreases by 58.2%, 34.4%, and 23.2% for the 20, 40, and 60 mm/hour rainfall scenario, respectively.

Keywords: fluvial flooding, pluvial flooding, hydraulic modeling, flood hazard, Slovakia

INTRODUCTION

Mapping fluvial and pluvial flood hazard is essential for effective flood risk management. It focuses on delineation of flood-prone zones and prediction of potential inundation, supporting decision-makers in implementing mitigation strategies and planning resilient infrastructure (Schanze, 2006; Vojtek et al., 2023).

Fluvial floods, represented by riverine and flash floods, arise when flood water level exceeds channel capacity and overflows onto surrounding floodplain. Riverine floods result from long-term rainfall or snowmelt, while flash floods are driven by short and intense rainfall (Maranzoni et al., 2023). Pluvial floods, or surface water flooding, occur when intense rainfall exceeds the infiltration or drainage capacity of sur-

✉e-mail: mvojtek@ukf.sk

faces or urban systems. They are independent of rivers or lakes and can occur anywhere on slopes or flat terrains, and they are particularly dangerous in urban areas with inadequate drainage infrastructure (Rözer et al., 2019).

Studies focusing on fluvial flood hazard are well represented in the literature (Beevers et al., 2020; Vojtek et al., 2024). In contrast, only a limited number of studies present a comprehensive analyses that specifically address pluvial flood hazard (Rözer et al., 2021; Mediero et al., 2022; Chano et al., 2025). Yet, pluvial flooding can pose economic risks comparable to those of fluvial flooding, especially in urban environments (Tanaka et al., 2020). Furthermore, several recent studies have explored the compound effects of fluvial and pluvial flood hazards (Rizeei et al., 2019; Bates et al., 2021; Xu et al., 2023; Cea et al., 2025).

Different approaches can be adopted for mapping fluvial and pluvial flooding inundation. The traditional approach is the physically-based, i.e. hydrologic-hydraulic, while the other approaches rely on geographic information system (GIS) and/or remote sensing (RS) techniques (Teng et al., 2017; Mudashiru et al., 2021). These approaches offer distinct modeling procedures for estimating flood extent, flow depth and velocity, each with their own advantages and limitations (Chlumsky et al., 2025; Vojtek et al., 2025).

The most accurate method for delineating flood extent and estimating flow depth is considered the physically-based (hydrologic-hydraulic) approach. The hydrologic component determines design discharges or hydrographs for specific return periods, which serve as upstream boundary conditions for the hydraulic model. The hydraulic component simulates the progress of flood discharge or flood wave through the channel and floodplain (Sciuto et al., 2025).

One-dimensional (1D) and two-dimensional (2D) hydraulic models are most commonly employed, each having different fundamentals and level of complexity (Dimitriadis et al., 2016; Arash and Yasi, 2022). Moreover, coupling 1D and 2D models is also possible (Vozinaki et al., 2016; Zandsalimi et al., 2024). In case of complex terrains and urban settings, 2D hydraulic models, which solve shallow water equations across a computational mesh, are preferred over 1D models (Vojtek and Vojteková, 2026). Owing to their higher numerical complexity, 2D models generally require longer computation time than 1D models.

The main aim of this article is to model fluvial and pluvial flood extents and flow depths using a 2D hydraulic approach, in particular the MIKE+ model, and geographic information systems under different scenarios. In particular, we investigated two partial objectives for the presented case study:

- Comparison and quantitative assessment of our hydraulic modeling results with the official fluvial flood maps for Q_{10}, Q_{100}, and Q_{1000} flood scenarios.
- Comparison and quantitative assessment of pluvial flood inundation maps for three net rainfalls (20, 40, and 60 mm/hour) under fully saturated soils scenario and scenario based on infiltration losses.

The novelty of this study for the Slovak scientific community lies in the fact that, to the best of our knowledge, no research, except those from the authors, has applied the MIKE+ model in the territory of Slovakia to date. The model has not been used for either fluvial or pluvial flood mapping. From this perspective, we present a case study demonstrating how the MIKE+ model can be applied in similar study areas across Slovakia using similar fluvial and pluvial flood inundation scenarios.

MATERIAL AND METHODS

Study area

The study area was located in the municipality of Sobotište, in western Slovakia, covering an area of 3.76 km^2 and including a 3.68 km long section of Teplica River. The area's elevation ranges from 231.3 to 376.7 m a. s. l. (Fig. 1a). The bed slope of the studied river section is 0.005 m/m. Since the studied area has been affected several times by fluvial and pluvial floods in the past, it is classified as a critical area for fluvial flooding, as determined by the most recent Preliminary Flood Risk Assessment cycle from 2024 (PFRA, 2024), carried out by the Ministry of Environment of the Slovak Republic under the EU Floods Directive (2007). Previous floods, especially those causing damage to assets, were the fluvial floods from 1997, 1999, 2005, 2006, 2009, and 2010. The last fluvial flood occurred on 15 September 2024 with a peak discharge equivalent to a return period of approximately 30 years.

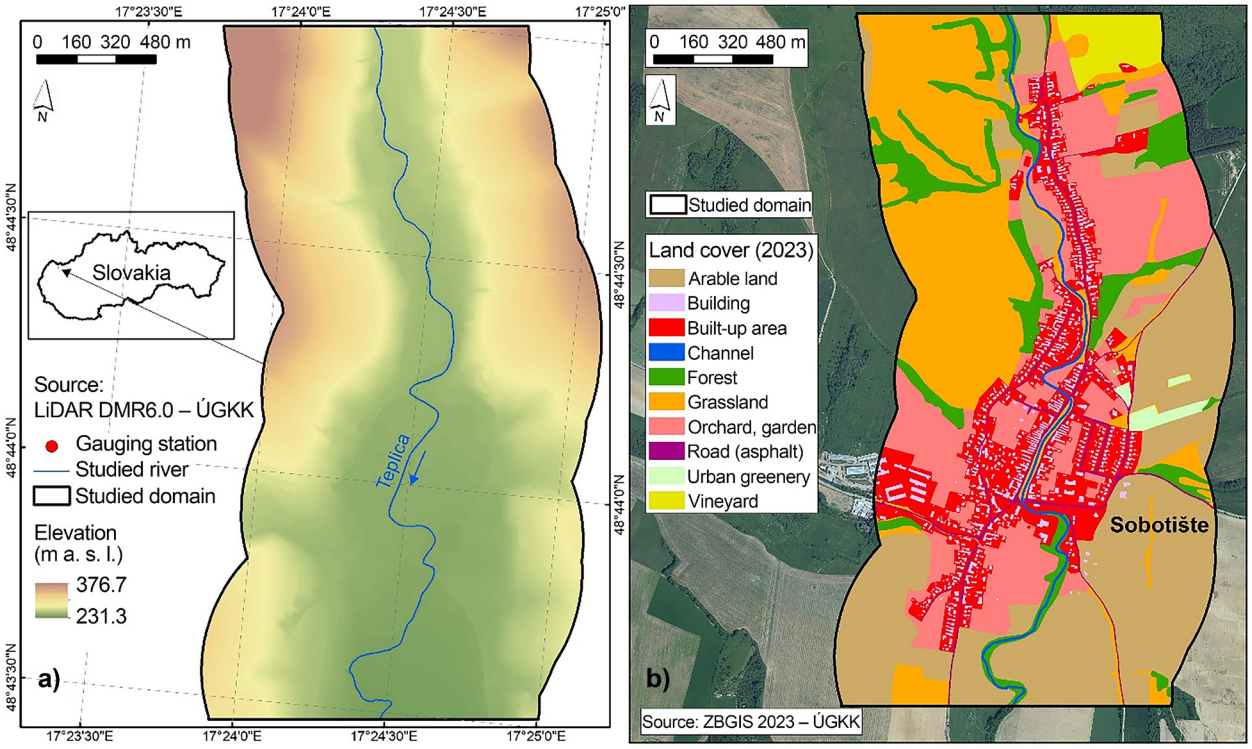

Fig. 1. Study area: a) elevation, b) land cover (Source: own elaboration)

The share of land cover classes from 2023 on the study area is as follows (Fig. 1b): arable land (30.5%), grassland (22.6%), orchard/garden (17.4%), built-up area (12.5%), forest (7.7%), building (3.7%), vineyard (2.3%), asphalt roads (1.7%), river channel (1.0%), and urban greenery (0.6%).

Data

Several types of input data were required for the hydraulic modeling of fluvial and pluvial floods, which were mainly processed in GIS. The airborne laser scanned (LiDAR) digital elevation model (DEM) with a resolution of 50 cm was available via the Geodetic and Cartographic Institute. The parameters of two bridges located on the river section were collected during a field survey along with the measured cross-sections, which were inserted into the DEM as bathymetry. The land cover of the study area was processed from the basic database for geographic information system (ZBGIS) from 2023, provided by the Geodetic and Cartographic Institute. The subsequent initial assignment of Manning's *n* roughness values was done following the work by Chow (1959), while the infiltration losses for individual land cover classes were assigned based on work of Rahmati et al. (2018). Table 1 presents the initially assigned Manning's *n* roughness values and the infiltration losses of land cover classes.

Table 1. Manning's *n* roughness values and the infiltration losses of land cover classes

Land cover class	Manning's *n* values ($s/m^{1/3}$)	Infiltration rate (mm/h)
Arable land	0.035	10
Building	1.00	1
Built-up area	0.04	5
Channel	0.04	0
Forest	0.15	40
Grassland	0.05	30
Orchard, garden	0.07	20
Road (asphalt)	0.02	1
Urban greenery	0.05	20
Vineyard	0.035	10

The fluvial flood models were calibrated by varying roughness coefficients until the maximum water stage value was reached during the fluvial flood from 18 March 2005. the Sobotište gauging station recorder its peak discharge at the rate of 26.56 m^3/s (Q_{10}). The adjusted roughness coefficient of the channel after calibration was 0.048, which matched to the measured water stage of 249 cm during this flood most closely. We used the calibrated Manning's *n* roughness coefficient from this flood event also for the rest of flood scenarios (Q_{100} and Q_{1000}), as reliable water stage data was available for these two flood scenarios. For the comparison of the modeled fluvial flood extent and flow depths, we used official flood maps for the same flood scenarios (Q_{10}, Q_{100}, and Q_{1000}) created by the Slovak Water Management Enterprise under the second cycle of the EU Floods Directive (2007). In the absence of spatially coherent field or remote sensing data necessary for validation, the results of the hydraulic modeling were instead assessed based on photographs taken during the last fluvial flood on 15 September 2024 in the study area. The fluvial flood of 15 September 2024 corresponds to a return period of approximately 30 years. The peak discharge measured at the Sobotište gauging station was 42.28 m^3/s. For validation purposes, we modeled this scenario too, using the same parametrization as for the other modeled flood scenarios. We then compared the flood extent for a particular river section depicted in the photographs with the modeled flood extent. In the case of pluvial flood models, there were no reliable records or data against which we could compare our modeling results.

Methods

In this article, we employed the two-dimensional (2D) hydraulic approach under the integrated MIKE+ interface. Some previous studies used MIKE+ (Welten et al., 2024) or its older version MIKE Flood (Ho et al., 2023; Wang et al., 2023; Xu et al., 2023) to model fluvial or pluvial floods. A specific MIKE Zero application was used to generate a flexible mesh. A triangular mesh with a maximum element area of 9 m^2 was created for floodplain, while a quadrangular mesh with the maximum lengths of 5 m in the stream direction and 2 m in the transversal direction was used for the river channel. The total number of mesh elements was 615,654. The minimum and maximum mesh element sizes were 0.54 and 18 m^2, respectively. Due to the unavailability of measured data, the water level for the downstream boundary condition was estimated by prolonging the length of the river reach far enough downstream to eliminate potential uncertainty in raising or lowering the resulting flow depth/surface water elevation. Initial conditions were set to a uniform water level of 229.2 cm. Further information on the applied 2D numerical scheme and water equations can be found in the MIKE+ documentation (https://manuals.mikepoweredbydhi.help/2025/MIKEPlus.htm#Documentation). In case of fluvial flood models, steady-state flow conditions were used to model maximum discharges with return periods of 10, 100, and 100 years, with the values of 26.8, 75, and 120 m^3/s, respectively. These maximum discharges represented the officially estimated values provided by the Slovak Hydrometeorological Institute.

In terms of pluvial flood modeling, we employed the rain-on-grid method with three modeled rainfall scenarios (20, 40, and 60 mm/hour) under the fully saturated soil conditions. Moreover, we also modeled the same three rainfall scenarios with infiltration losses for each land cover class. The Manning's *n* roughness values were used in the same way as for fluvial flooding. For both model types, the 2D overland hydrodynamic solver was used, with the maximum CFL factor value of 0.8. The simulation time step was set to 10 seconds, as this is a common and recommended value by DHI for detailed yet efficient simulations aiming to achieve numerical stability in the model. The simulation time was 3 hours for fluvial flooding and 30 minutes for pluvial flooding.

To evaluate quantitative differences between the modeled flood extents and official flood, five metrics (critical success index – CSI, bias, recall, precision, and F1-score) were calculated using the following equations (1–5) (Vojtek et al., 2025):

$$CSI = \frac{TP}{TP + FP + FN} \tag{1}$$

$$\text{Bias} = \frac{TP + FP}{TP + FN} \tag{2}$$

$$\text{Recall} = \frac{TP}{TP + FN} \tag{3}$$

$$\text{Precision} = \frac{TP}{TP + FP} \quad (4)$$

$$\text{F1} - \text{score} = \frac{2 \cdot \text{Precision} \cdot \text{Recall}}{\text{Precision} + \text{Recall}} \quad (5)$$

where TP, FP, and FN are true positive, false positive, and false negative areas (in m^2), respectively. True positive represents areas where the modeled and official flood extent are the same. False positive are modeled areas outside the official flood extent. False negative are areas with no flood extent modeled by the MIKE+ model inside the official flood extent maps. Regarding the evaluation of overlapping flow depth pixels between modeled and official maps, these four metrics were used: root mean square error (RMSE), mean absolute error (MAE), mean error (ME), and standard deviation (SD).

RESULTS

Fluvial flood inundation

The modeled flood extent for the Q_{10} flood scenario yielded a total area of 59,303 m^2. This is 8,268 m^2 less than the area in the official Q_{10} flood map, a result that was also confirmed by the calculated metrics. The TP, FP, and FN areas were 56,406.25, 2,896.75, and 11,164.58 m^2, respectively. The resulting comparative metrics had the values of 0.800, 0.878, 0.835, 0.951, and 0.889 for the CSI, bias, recall, precision, and F1-score metric, respectively. Regarding the Q_{10} flood scenario, the values of 0.37 (RMSE), 0.29 (MAE), −0.17 (ME), and 0.32 (SD) were recorded when comparing the flow depth difference (Table 2).

The percentage share of flow depth intervals for Q_{10} flood scenario is shown in Figure 2a. A similar proportion of flow depth pixels was recorded in the first four intervals (around 21–26%), while the flow depth pixels in the last interval (2.0–2.6 m) accounted for only 5.4% of pixels. Figure 2b illustrates the differences in flow depths between the modeled and the official flood map. The highest percentage of flow depth differences occurred between –0.50–0.50 m (83.6%) and between –1.00– –0.50 (14.1%). The other intervals of flow depth differences represented around 1% or less of overlapping flood extent.

As for the modeled flood extent for the Q_{100} flood scenario, the calculated total area was 264,019 m^2, which is less by 75,581 m^2 than in the official Q_{100} flood map. The area of TP, FP, and FN resulted in the values of 257,337.45, 6,681.50, and 82,262.59 m^2, respectively. The resulting comparative metrics had the values of 0.743, 0.777, 0.758, 0.975, and 0.853 for the CSI, bias, recall, precision, and F1-score metric, respectively.

Table 2. Comparison metrics for the modeled vs. the official flood extent and flow depth for the studied flood scenarios

Q_{10}												
Modeled extent (m^2)	TP (m^2)	FP (m^2)	FN (m^2)	CSI	Bias	Recall	Precision	F1-score	RMSE	MAE	ME	SD
59,303	56,406.25	2,896.75	11,164.58	0.800	0.878	0.835	0.951	0.889	0.368	0.289	–0.174	0.324
Q_{100}												
Modeled extent (m^2)	TP (m^2)	FP (m^2)	FN (m^2)	CSI	Bias	Recall	Precision	F1-score	RMSE	MAE	ME	SD
264,019	257,337.75	6,681.50	82,262.59	0.743	0.777	0.758	0.975	0.853	0.283	0.190	–0.135	0.249
Q_{1000}												
Modeled extent (m^2)	TP (m^2)	FP (m^2)	FN (m^2)	CSI	Bias	Recall	Precision	F1-score	RMSE	MAE	ME	SD
423,159	414,545.25	8,613.25	131,947.56	0.747	0.774	0.759	0.980	0.855	0.307	0.214	–0.169	0.255

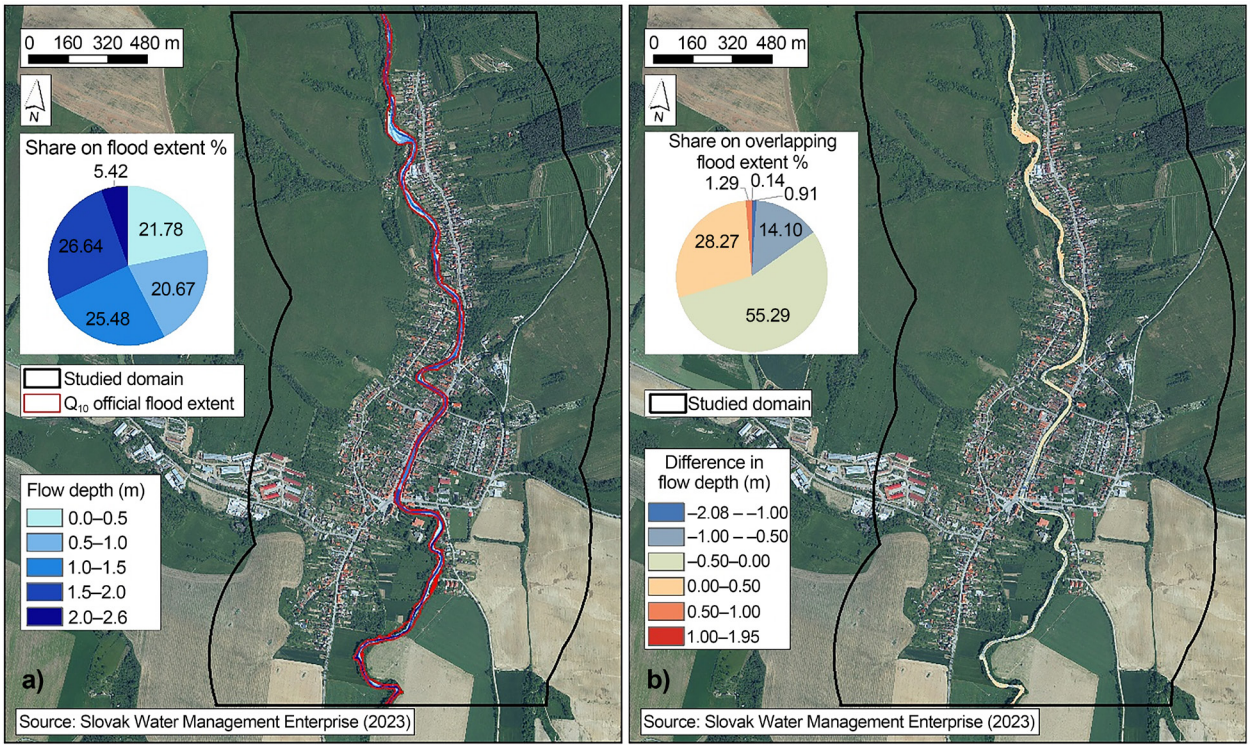

Fig. 2. Q_{10} fluvial flood scenario: a) modeled flow depths and official flood extent and b) difference in flow depths between modeled and official maps (Source: own elaboration)

As for the Q_{100} flood scenario, the values of 0.28 (RMSE), 0.19 (MAE), −0.14 (ME), and 0.25 (SD) were achieved when comparing the flow depth difference (Table 2).

The calculated percentage share of flow depth intervals for the Q_{100} flood scenario (Fig. 3a) was as follows. Most of the pixels (63.3%) fell into the first interval 0.0–0.5 m. A similar proportion of pixels (12.7% and 12.8%) was recorded in the second (0.5–1.0 m) and last interval (2.0–3.6 m). The smallest percentage of pixels was in the third (1.0–1.5 m) and fourth (1.5–2.0 m) interval, with percentage values of 6.2% and 5.1%, respectively. Figure 3b presents the difference in flow depths between the modeled and the official flood map. The highest percentage difference in flow depth was recorded in the interval –0.50–0.50 m (91.9%) and interval –1.00– –0.50 (6.6%). The other flow depth difference intervals demonstrated around 1% or less of overlapping flood extent.

In case of the modeled flood extent for the Q_{1000} flood scenario, the calculated total area was 423,159 m^2, which is less by 123,334 m^2 than in the official Q_{1000} flood map. The area of TP, FP, and FN resulted in the values of 414,545.25, 8,613.25, and 131,947.56 m^2, respectively. The resulting comparative metrics had the values of 0.747, 0.774, 0.759, 0.980, and 0.855 for the CSI, bias, recall, precision, and F1-score metric, respectively. In case of the Q_{1000} flood scenario, the values of 0.31 (RMSE), 0.21 (MAE), −0.17 (ME), and 0.26 (SD) were recorded when comparing the flow depth difference (Table 2).

The calculated percentage share of flow depth intervals for the Q_{1000} flood scenario (Fig. 4a) recorded similar values as in case of the Q_{100} flood scenarios. Most of the pixels (64.9%) fell into the first interval 0.0–0.5 m. A similar proportion of pixels (14.5% and 10.8%) was recorded in the second (0.5–1.0 m) and last interval (2.0–4.1 m). The smallest percentage of pixels was in the third (1.0–1.5 m) and fourth (1.5–2.0 m) interval with percentage values of 6.0% and 3.7%, respectively. Figure 4b shows difference in flow depths between modeled and official flood maps.

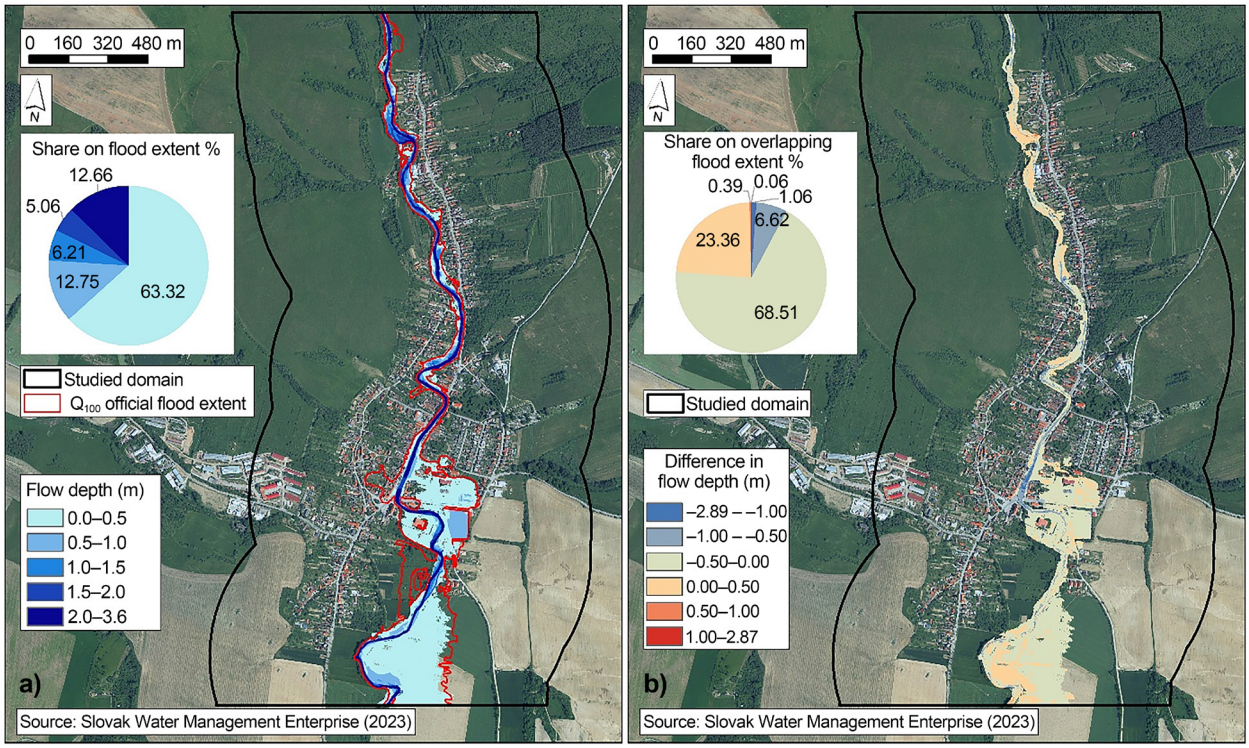

Fig. 3. Q_{100} fluvial flood scenario: a) modeled flow depths and official flood extent and b) difference in flow depths between modeled and official maps (Source: own elaboration)

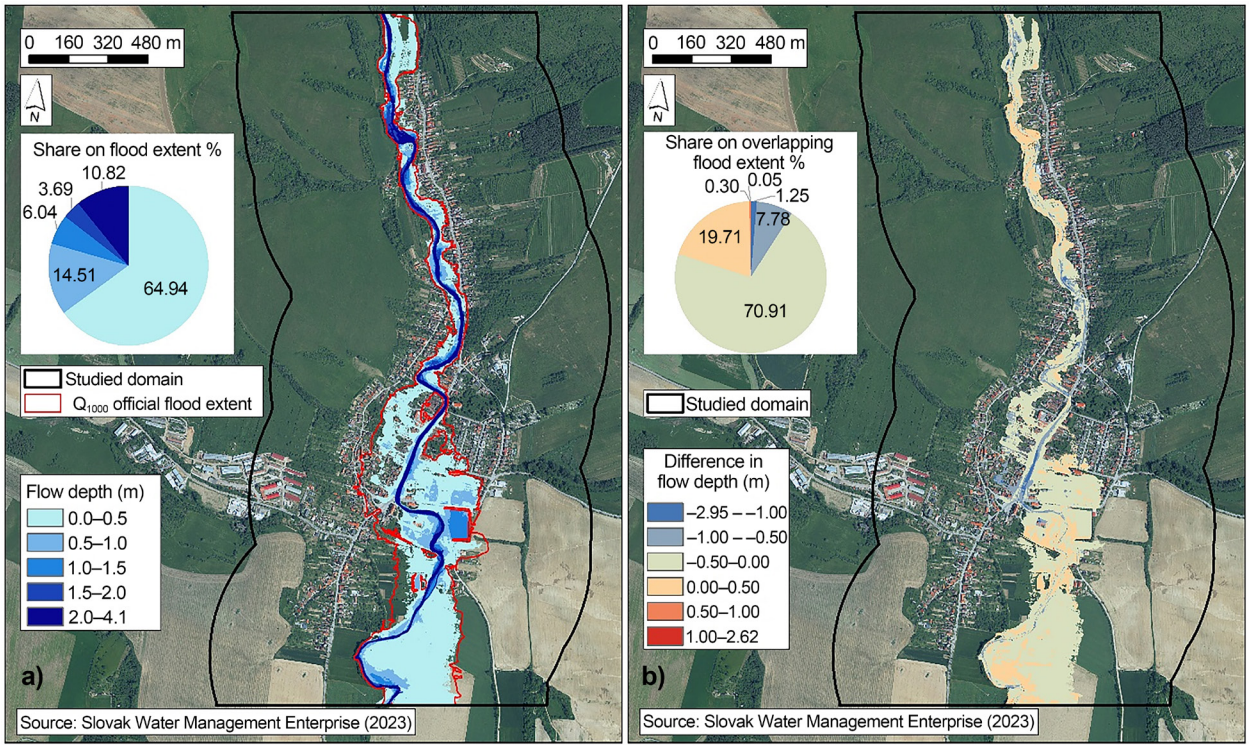

Fig. 4. Q_{1000} fluvial flood scenario: a) modeled flow depths and official flood extent and b) difference in flow depths between modeled and official maps (Source: own elaboration)

The highest percentage difference in flow depth was recorded between –0.50 and 0.50 m (90.6%) and between –1.00 and –0.50 (7.8%). The other flow depth difference intervals reached around 1% or less of the overlapping flood extent.

Validation of the modeled Q_{30} fluvial flood on 15 September 2024 in Sobotište is presented in Figure 5. Although this is only a short section of the modeled river, there is a good agreement between the modeled and the actual flood extents during this flood event.

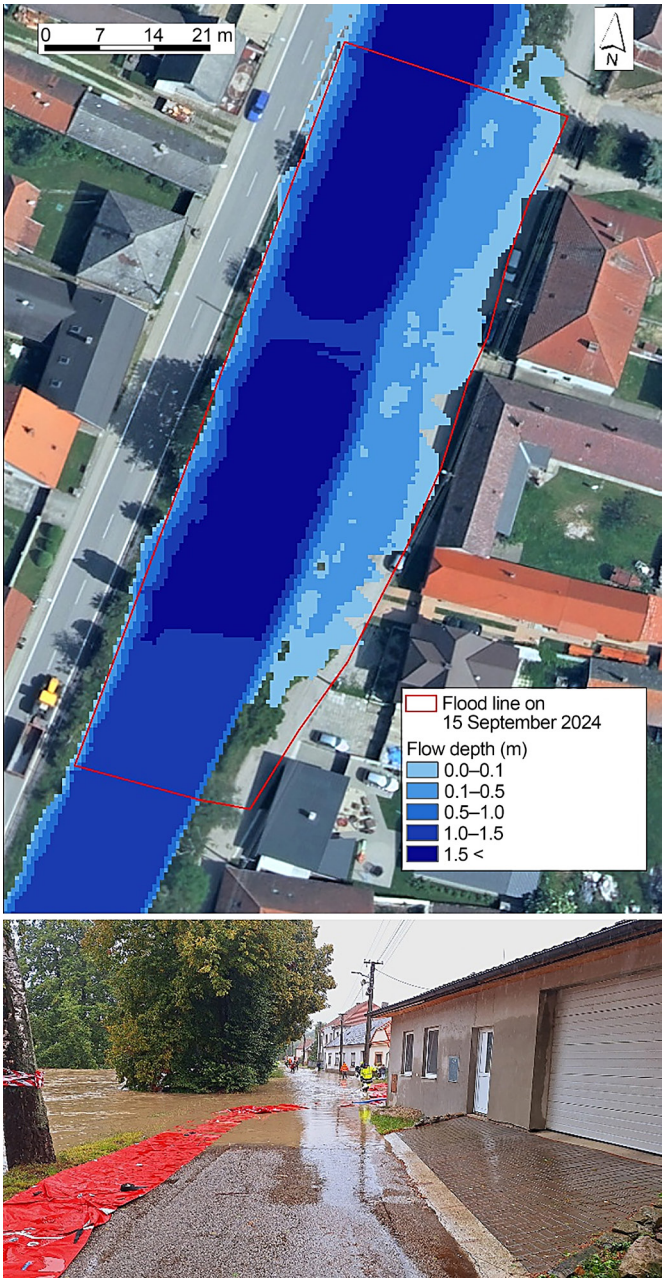

Fig. 5. Validation of flood lines caused by the fluvial flood on 15 September 2024 based on photograph taken in the Sobotište municipality during this flood (Source: own elaboration)

Pluvial flood inundation

Regarding the pluvial flooding scenario involving net rainfall and fully saturated soils at the intensity of 20 mm/hour, most of the pixels (84.4%) in the study area were categorised as non-flooded areas, as they had flow depths less than 0.005 m. The flood extent was 0.55 km^2. The percentage share of flow depth intervals that were higher than 0.005 m in the 20 mm/hour rainfall scenario were classified as flooded. The largest proportion of pixels (7.8%) of the total area extent fell into the second interval 0.01–0.05 m, followed by the first interval (0.005–0.01 m) and the third interval (0.05–0.10 m), which accounted for 3.5% and 2.2% of pixels, respectively. The least percentage of pixels occurred in the fourth (0.10–0.50 m) and fifth (0.50–1.36 m) intervals with percentage values of 1.8% and 0.2%, respectively (Fig. 6a).

In case of the pluvial flooding scenario involving a net rainfall of 20 mm/hour, incorporating infiltration losses, most pixels (93.4%) in the study area were classified as non-flooded, as they had flow depths less than 0.005 m. The flood extent covered 0.23 km^2. The percentage share of flow depth intervals that were higher than 0.005 m were classified as flooded. The largest proportion of pixels (3.6%) of the total area extent fell into the second interval 0.01–0.05 m, followed by the first (0.005–0.01 m) and the third (0.05–0.10 m) intervals, which accounted for 1.5% and 0.9% of pixels, respectively. The least percentage of pixels occurred in the fourth (0.10–0.50 m) and the fifth (0.50–1.36 m) intervals with percentage values of 0.4% and 0.001%, respectively (Fig. 6b).

As in the previous rainfall scenario with fully saturated soils, the majority of pixels in the study area in the case of a 40 mm/hour rainfall scenario were classified as non-flooded, as they had flow depths below 0.005 m (73.7%). The flood extent was 0.93 km^2. The percentage share of flow depth intervals that were higher than 0.005 m for the 40 mm/hour rainfall scenario were classified as flooded. The largest proportion of the pixels (12.0%) of the total area extent fell into the second interval 0.01–0.05 m, followed by the first

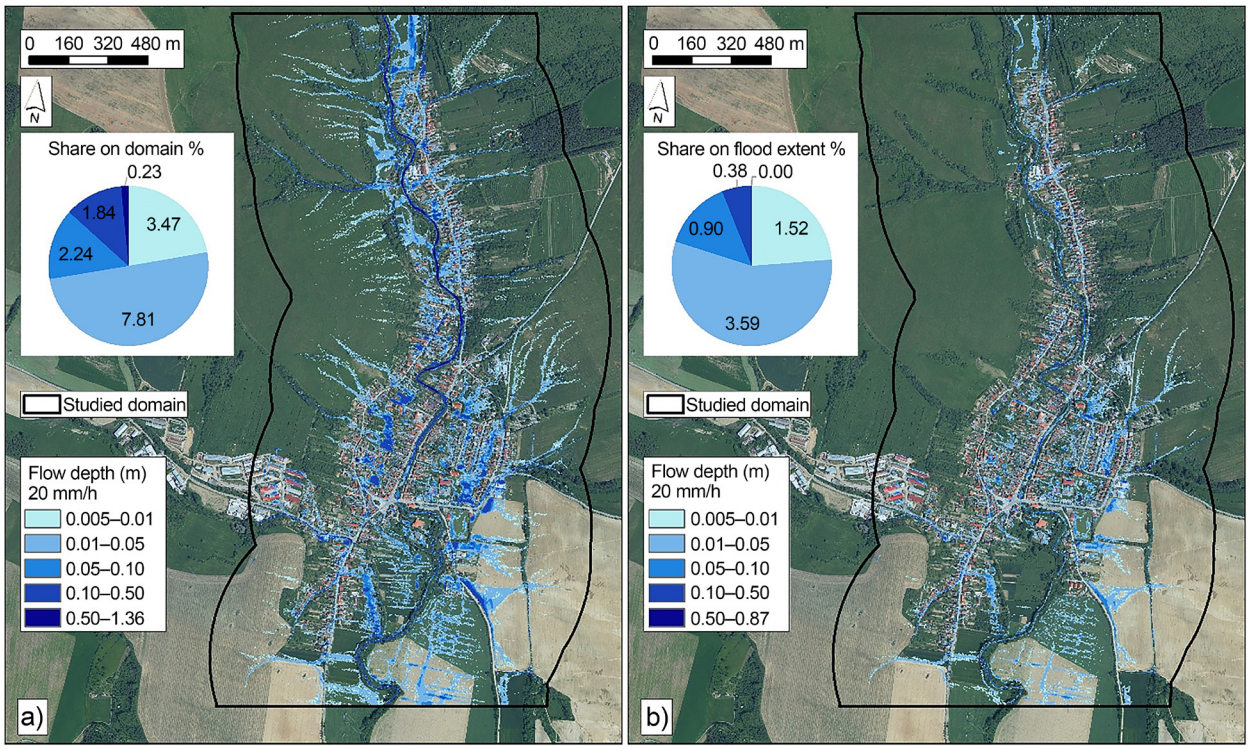

Fig. 6. Pluvial flood scenario with the rainfall intensity of 20 mm/hour: a) modeled flow depths under fully saturated soils and b) modeled flow depths with infiltration losses (Source: own elaboration)

(0.005–0.01 m), and the third (0.05–0.10 m) intervals, with values of 6.6% and 3.5%, respectively. The least percentage of pixels was in the fourth (0.10–0.50 m) and the fifth (0.50–1.59 m) intervals, with percentage values of 3.4% and 0.8%, respectively (Fig. 7a).

In case of the pluvial flooding scenario involving net rainfall of 40 mm/hour, incorporating infiltration losses, most pixels (82.9%) in the study area were classified as non-flooded, as they had flow depths below 0.005 m. The flood extent was 0.61 km^2. The percentage share of flow depth intervals that were higher than 0.005 m were classified as flooded. Most pixels (8.3%) of total area extent fell into the second interval 0.01–0.05 m, followed by the first (0.005–0.01 m) and the third (0.05–0.10 m) intervals, with values of 3.8% and 2.5%, respectively. The least percentage of pixels was in the fourth (0.10–0.50 m) and the fifth (0.50–1.36 m) intervals, with percentage values of 2.4% and 0.2%, respectively (Fig. 7b).

In the case of 60 mm/hour rainfall scenario with fully saturated soils, the majority of the pixels in the study area were classified as non-flooded, as they had flow depths below 0.005 m (64.7%). The flood extent covered 1.25 km^2. The percentage share of flow depth intervals that were higher than 0.005 m for the 60 mm/hour rainfall scenario were classified as flooded. Most pixels (15.7%) of the total area extent fell into the second interval 0.01– 0.05 m, followed by the first (0.005–0.01 m) and the fourth (0.0– 0.10 m) intervals, with values of 9.0% and 4.7%, respectively. The least percentage of pixels was in the third (0.10–0.50 m) and the fifth (0.50–2.08 m) intervals, with percentage values of 4.5% and 1.4%, respectively (Fig. 8a).

Regarding the pluvial flooding scenario involving the net rainfall of 40 mm/hour, incorporating infiltration losses, most pixels (72.8%) in the study area were classified as non-flooded, as they had flow depths below 0.005 m. The flood extent covered 0.96 km^2. The percentage share of flow depth intervals that were higher than 0.005 m were classified as flooded. Most pixels (12.3%) of the total area extent fell into the second interval 0.01–0.05 m, followed by the first

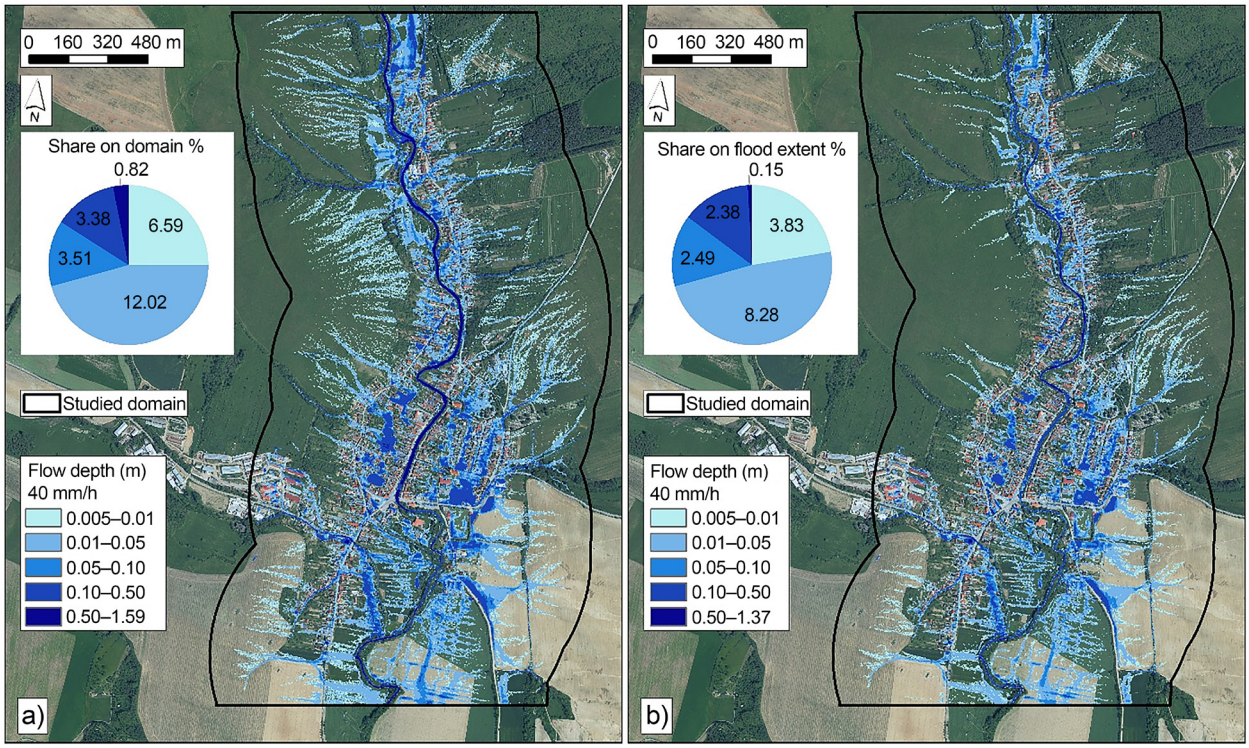

Fig. 7. Pluvial flood scenario with the rainfall intensity of 40 mm/hour: a) modeled flow depths under fully saturated soils and b) modeled flow depths with infiltration losses (Source: own elaboration)

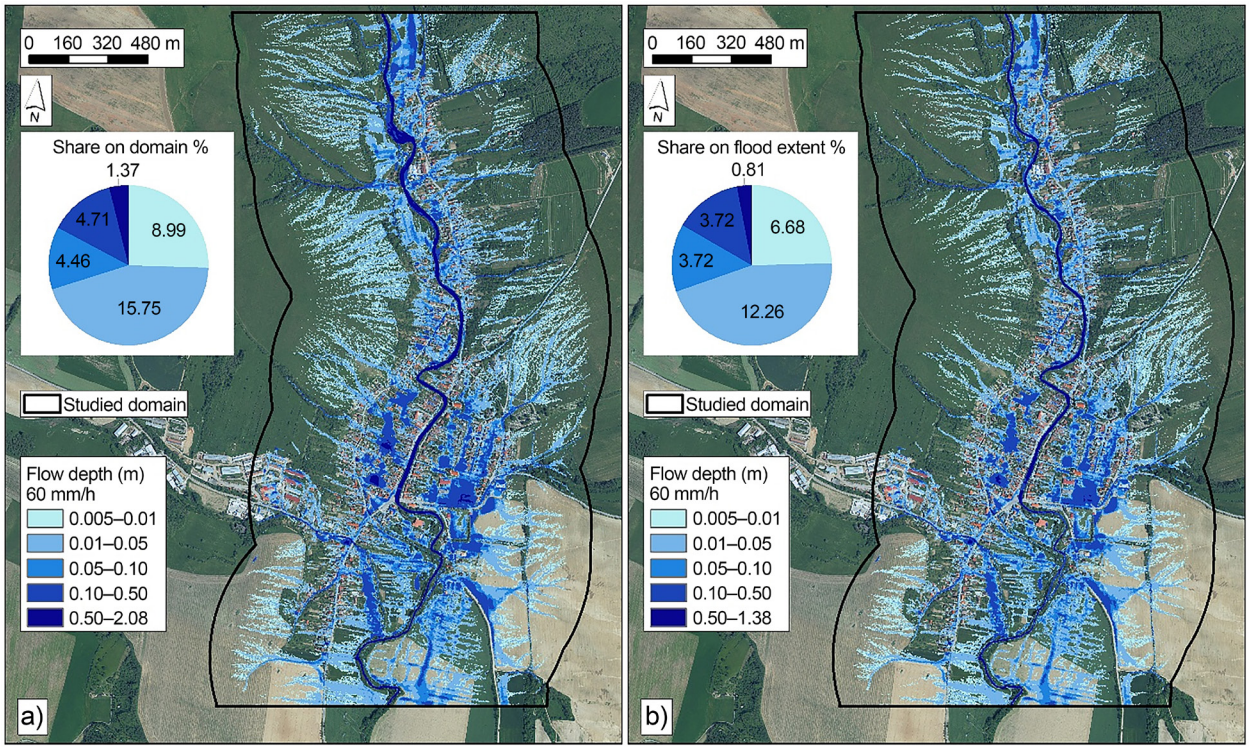

Fig. 8. Pluvial flood scenario with the rainfall intensity of 60 mm/hour: a) modeled flow depths under fully saturated soils and b) modeled flow depths with infiltration losses (Source: own elaboration)

(0.005–0.01 m) and the third (0.05–0.10 m) intervals, with values of 6.7% and 3.7%, respectively. The least percentage of pixels was in the fourth (0.10–0.50 m) and the fifth (0.50–1.36 m) intervals, with percentage values of 3.7% and 0.8%, respectively (Fig. 8b).

DISCUSSION

Flood hazard mapping or inundation modelling, whether fluvial or pluvial, are covered by one of the Sustainable Development Goals (SDGs) set by the United Nations. More specifically, it falls under the Climate Action goal, which prioritizes taking measures to address climate change and its impacts, such as the occurrence of natural hazards (in this case specifically floods) worldwide.

This study highlights the capacity of the MIKE+ modeling framework to simulate fluvial and pluvial flooding through physically-based hydraulic representations. The calibrated 2D overland MIKE+ model was able to represent the river overbank inundation, yet it underestimates the official flood extents for the studied flood scenarios. Pluvial flooding was simulated using the same 2D overland solver in the MIKE+ model with rainfall inputs for fully saturated soils and with infiltration losses. This enabled direct representation of overland flow for these two variants. This approach is consistent with other pluvial flood studies that emphasize the advantages of fully two-dimensional hydraulic models over simplified runoff routing techniques (Bao et al., 2017; Yang et al., 2020). The results indicate that the 2D MIKE+ model effectively captures major pluvial flow paths and accumulation zones, particularly in varying terrain. Using high-resolution DEM (0.5 m resolution) ensures that micro-topographic features influencing shallow overland flow, such as road cambers and small embankments, were resolved, leading to localized representation of flow depths. The necessity of high-resolution input data for hydraulic modeling of fluvial and pluvial flooding was also confirmed by Chano et al. (2025) and Sañudo et al. (2025).

Despite its advanced capabilities, the MIKE+ modeling framework is subject to uncertainties related to parameter selection, boundary conditions, and input data quality. Pluvial flood simulations are particularly sensitive to rainfall intensity, which emphasizes the importance of high-resolution rainfall data for urban flood modeling. Additionally, the absence of constructed stormwater drainage networks in the studied urbanized parts of the municipality led to significant surface flooding, which was also pointed out by Montalvo et al. (2024).

The generated flood extent and flow depth maps were compared with the officially modeled flood extents produced during the second cycle of the EU Floods Directive (2007) implementation. It should be noted that only limited information about the official flood hazard maps was available, which was a limitation for the research. The official flood maps were developed using the 2D hydraulic modeling approach, i.e. the MIKE+ model with the same numerical scheme, under steady-state flow conditions for design discharges corresponding to 10-, 100-, and 1000-year return periods.

However, input data, like DEM, and key model parameters, such as roughness coefficients, hydraulic structures, boundary conditions, and mesh generation details, were not accessible. Although these parameters are documented in the technical reports accompanying the official flood maps and were formally requested from the Slovak Water Management Enterprise, the request was denied. Consequently, model comparison was performed using the flood extent polygons as well as flow depths for the same 10-, 100-, and 1000-year return periods.

The calibrated channel value of 0.048, which corresponds to the water stage during the flood on 18 March 2005, was also used for the other flood scenarios. The reason for this is there are no measured records of water stages or discharges at the Sobotište gauging station, which could have been used for the calibration of Q_{100} and Q_{1000}. As confirmed by Ardiçlioğlu and Kuriqi (2019), estimating the roughness of a channel is one the most challenging procedures in developing hydraulic models for flood prediction and flood hazard mapping. The calibration process used in this study could have influenced the resulting flood extent for Q_{100} and Q_{1000} flood scenarios. Compared to the official flood maps, these scenarios recorded lower values of CSI and bias than the Q_{10} scenario. However, we must also raise a question whether (and how) the official flood maps for the Q_{100} and Q_{1000} flood scenarios were calibrated and validated, as no such flood occurred in the last 30–40 years of well-documented discharges in the study area.

Furthermore, the decrease in performance metrics, such as CSI and recall, with higher return periods was due to a mixture of model parameter settings and input data, which we believe were different in the official flood maps. As we are unaware of the exact model parametrization and use of input data, we assume that the most influential parameter propagating the difference was roughness, probably with higher Manning's *n* values. Liu et al. (2019) found out that the performance of 2D models improves with increasing channel roughness, enabling more water to enter the floodplain. In addition, we hypothesize that the generated mesh was coarser, with a lower number of elements and a larger element size, as a much longer section of the Teplica River was simulated in the official flood mapping than in this study. Hoch et al. (2018) found out that coarser mesh tends to predict larger inundation extent on floodplains. All in all, the parameters that were the same as in the official flood maps were the return periods, steady-state flow conditions, and the 2D overland solver in the MIKE+ model.

We also acknowledge the limitations of validation data for pluvial flooding, given that no such data were available. Therefore, future research has to focus on obtaining more reliable and spatially coherent validation data for both types of floods. In particular, the validation data for pluvial flooding need to be obtained during or shortly after the actual pluvial events, utilizing also citizen reports/photographs, post-event surveys, or satellite-based flood detection. Incorporating climate change scenarios into the models with varying rainfall inputs under optimistic, neutral, and pessimistic scenarios can be also included into future research. In addition to the already mentioned future directions, uncertainty/sensitivity analysis, for example with regard to DEM resolution, roughness values, infiltration rates, or simulation times, could also provide useful information to improve the modeling results. Future research should plan using the validated fluvial and pluvial flood maps for further training of the machine/deep learning models, so that the flood extent as well as

flow depths can be extrapolated to other sections of the studied river, as well as to other (similar) study areas.

CONCLUSIONS

Based on the results achieved, we can summarize that the 2D MIKE+ hydraulic model yielded significant fluvial flooding risk for Q_{100} and Q_{1000} flood scenarios, while for the Q_{10} flood scenario, it has revealed relatively low flood hazard in the studied area. Moreover, the modeled fluvial flood extents underestimated the flood extents in the official flood maps for all flood scenarios. The underestimation of modeled flood extents, compared to the official flood maps, increases from the Q_{10} to the Q_{1000} flood scenario. The highest percentage of flow depth difference was recorded in the intervals –0.50–0.50 m and –1.00– –0.50 m for all flood scenarios. It has to be noted that due to lack of detailed information on the modeling procedure and input data used for the creation of official flood maps, the models were only compared with respect to the flood extent polygons and rasters of flow depths corresponding to the same return periods of 10, 100, and 1000 years.

Furthermore, under the modeled net rainfall scenarios (20, 40, and 60 mm/hour), the study area could be significantly influenced by pluvial flooding, when the soils are fully saturated. The share of flow depths higher than 0.005 m at the total pluvial flood extent increases with the increasing rainfall amounts. When counting with the infiltration rates of individual land cover classes, pluvial flood extent decreases by 58.2%, 34.4%, and 23.2% for the 20, 40, and 60 mm/hour rainfall scenario, respectively.

The presented results emphasize the need for assessing pluvial flood hazards along with fluvial ones. Official flood hazard maps, created under the EU Floods Directive (2007), only show fluvial flood hazard. However, there is also a need for assessing potential pluvial flooding scenarios , which gradually gains the same importance as the fluvial flooding, specifically, in Slovakia.

ACKNOWLEDGMENT

Funded by the EU NextGenerationEU through the Recovery and Resilience Plan for Slovakia under the project No. 09I03-03-V03-00085.

REFERENCES

Arash, A.M., Yasi, M. (2022). The assessment for selection and correction of RS-based DEMs and 1D and 2D HEC-RAS models for flood mapping in different river types. Journal of Flood Risk Management, 16(1), e12871.

Ardıçlıoğlu, M., Kuriqi, A. (2019). Calibration of channel roughness in intermittent rivers using HEC-RAS model: case of Sarimsakli creek, Turkey. SN Applied Sciences, 1, 1080.

Bao, H., Wang, L., Zhang, K., Li, Z. 2017. Application of a developed distributed hydrological model based on the mixed runoff generation model and 2D kinematic wave flow routing model for better flood forecasting. Atmospheric Science Letters, 18(7), 284–293.

Bates, P.D., Quinn, N., Sampson, C., Smith, A., Wing, O., Sosa, J., Savage, J., Olcese, G., Neal, J., Schumann, G., Giustarini, L. (2021). Combined modeling of US fluvial, pluvial, and coastal flood hazard under current and future climates. Water Resources Research, 57(2), e2020WR028673.

Beevers, L., Collet, L., Aitken, G., Maravat, C., Visser, A. (2020). The influence of climate model uncertainty on fluvial flood hazard estimation. Natural Hazards, 104, 2489–2510.

Cea L., Sañudo, E., Montalvo, C., Farfán, J., Puertas, J., Tamagnone, P. (2025). Recent advances and future challenges in urban pluvial flood modelling. Urban Water Journal, 22(2), 149–173.

Chano, J.S.C., Brigandi, G., Aronica, G.T. (2025). Comparison of Pluvial Flooding Modeling Software Applied in Highly Urbanized Settlements Using the Case of Lake Ganzirri. Water, 17(20), 2978.

Chlumsky, R., Craig, J.R., Tolson, B.A. (2025). A reach-integrated hydraulic modelling approach for large-scale and real-time inundation mapping. Geoscientific Model Development, 18(11), 3387–3403.

Chow, V.T. (1959). Open-Channel Hydraulics. McGraw-Hill Higher Education, New York.

Dimitriadis, P., Tegos, A., Oikonomou, A., Pagana, V., Koukouvinos, A., Mamassis, N., Koutsoyiannis, D., Efstratiadis, A. (2016). Comparative evaluation of 1D and quasi-2D hydraulic models based on benchmark and real-world applications for uncertainty assessment in flood mapping. Journal of Hydrology, 534, 478–492.

EU Floods Directive (2007). Directive 2007/60/EC of the European Parliament and of the Council of 23 October 2007 on the Assessment and Management of Flood Risks. https://eur-lex.europa.eu/legal-content/EN/TXT/?

uri=CELEX%3A32007L0060&qid=1762372896195 [accessed 2025.10.25].

Ho, B.Q., Hguyen, T., Vu, K., Dao, K., Dung, N.A., Huynh, N. 2023. Apply MIKE models to study the impacts of climate change on flooding and design adaptation measures in Can Tho City in the Vietnamese Mekong Delta. IOP Conference Series: Earth and Environmental Science, 1247, 012016.

Hoch, J.M., Beek, R., Winsemius, H.C., Bierkend, M.F.P. 2018. Benchmarking flexible meshes and regular grids for large-scale fluvial inundation modelling. Advances in Water Resources, 121, 350–360.

Liu, Z., Merwade, V., Jafarzadegan, K. (2019). Investigating the role of model structure and surface roughness in generating flood inundation extents using one- and two--dimensional hydraulic models. Journal of Flood Risk Magement, 12, e12347.

Maranzoni, A., D'Oria, M., Rizzo, C. (2023). Quantitative flood hazard assessment methods: A review. Journal of Flood Risk Management, 16(1), e12855.

Mediero, L., Soriano, E., Oria, P., Bagli, S., Castellarin, A., Garrote, L. Mazzoli, P., Mysiak, J., Pasetti, S., Persiano, S., Santillán, D., Schröter, K. (2022). Pluvial flooding: High-resolution stochastic hazard mapping in urban areas by using fast-processing DEM-based algorithms. Journal of Hydrology, 608, 127649.

Montalvo, C., Reyes-Silva, J.D., Sañudo, E., Cea, L., Puertas, J. (2024). Urban pluvial flood modelling in the absence of sewer drainage network data: A physics-based approach. Journal of Hydrology, 634, 131043.

Mudashiru, R.B., Sabtu, N., Abustan, I., Balogun, W. (2021) Flood hazard mapping methods: A review. Journal of Hydrology 603, 126846.

PFRA (2024). Predbežné hodnotenie povodňového rizika v Slovenskej republike – aktualizácia 2024 [Preliminary Flood Risk Assessment in the Slovak Republic – Update 2024]. https://www.minzp.sk/files/sekcia-vod/ochrana--pred-povodnami/2025/predbezne-hodnotenie-povodnoveho-rizika-sr-2024/phpr_sr_2024.pdf, last [accessed 2025.10.25].

Rahmati et al. (2018). Development and analysis of the Soil Water Infiltration Global database. Earth System Science Data, 10(3), 1237–1263.

Rizeei, H.M., Pradhan, B., Saharkhiz, M.A. (2019). An integrated fluvial and flash pluvial model using 2D high-resolution sub-grid and particle swarm optimization-based random forest approaches in GIS. Complex & Intelligent Systems, 5, 283–302.

Rözer, V., Kreibich, H., Schröter, K., Müller, M., Sairam, N., Doss-Gollin, J., Lall, U., Merz, B. (2019). Probabilistic models significantly reduce uncertainty in Hurricane Harvey pluvial flood loss estimates. Earth's Future, 7(4), 384–394.

Rözer, V., Peche, A., Berkhahn, S., Feng, Y., Fuchs, L., Graf, T., Haberlandt, U., Kreibich, H., Sämann, R., Sester, M., Shehu, B., Wahl, J., Neuweiler, I. (2021). Impact--based forecasting for pluvial floods. Earth's Future, 9, e2020EF001851

Sañudo, E., Gabrcía-Feal, O., Hagen, L., Cea, L., Puertas, J., Montalvo, C., Alvarado-Vicencio, R., Hofmann, J. 2025. IberSWMM+: A high-performance computing solver for 2D-1D pluvial flood modelling in urban environments. Journal of Hydrology, 651, 132603.

Schanze, J. (2006). Flood risk management – a basic framework. In: Schanze, J., Zeman, E., Marsalek, J. (eds.) Flood risk management: hazards, vulnerability and mitigation measures, 1–20. Springer Netherlands, Houten.

Sciuto, L., Licciardello, F., Giuffrida, E.R., Barresi, S., Scavera, V., Verde, D., Barbagallo, S., Cirelli, G.L. (2025). Hydrological-hydraulic modelling to assess Nature-Based Solutions for flood risk mitigation in an urban area of Catania (Sicily, Italy). Nature-Based Solutions, 7, 100210.

Tanaka, T., Kiyohara, K., Tachikawa, Y. (2020). Comparison of fluvial and pluvial flood risk curves in urban cities derived from a large ensemble climate simulation dataset: A case study in Nagoya, Japan. Journal of Hydrology, 584, 124706.

Teng, J., Jakeman, A.J., Vaze, J., Croke, B.F., Dutta, D., Kim, S.J.E.M. (2017). Flood inundation modelling: A review of methods, recent advances and uncertainty analysis. Environmental Modelling & Software, 90, 201–216.

Vojtek, M., Vojteková, J., De Luca, D.L., Petroselli, A. (2023). Combined basin-scale and decentralized flood risk assessment: a methodological approach for preliminary flood risk assessment. Hydrological Sciences Journal, 63(3), 355–378.

Vojtek, M., Moradi, S., De Luca D.L., Petroselli, A., Vojteková, J. (2024). Fluvial and pluvial flood hazard mapping: combining basin and municipal scale assessment. Geomatics, Natural Hazards and Risk, 15(1), 2432377.

Vojtek, M., Moradi, S., Petroselli, A., Vojteková, J. (2025). Comparative analysis of hydraulic and GIS-based Height Above the Nearest Drainage model for fluvial flood hazard mapping: a case of the Gidra River, Slovakia. Stochastic Environmental Research and Risk Assessment, 39, 2657–2675.

Vojtek, M., Vojteková, J. (2026). Fluvial Flood Inundation Modeling: a Comparative Assessment of 1D and 2D Hy-

draulic Approach Using MIKE+. Water Resource Management, 40, 24.

Vozinaki, A.E.K., Morianou, G.G., Alexakis, D.D., Tsanis, I.K. (2016). Comparing 1D and combined 1D/2D hydraulic simulations using high-resolution topographic data: a case study of the Koiliaris basin, Greece. Hydrological Sciences Journal, 62, 642–656.

Wang, Z., Lyu, H., Zhang, C. 2023. Pluvial flood susceptibility mapping for data-scarce urban areas using graph attention network and basic flood conditioning factors. Geocarto International, 38(1), 2275692.

Welten, S., Holt, A., Weber, J., Klopiers, E.M., Schüttrumpf, H., Decker, S. 2024. Generation of harmonised pluvial flood hazard maps through decentralised analytics. Journal of Hydroinformatics, 26(2), 534–548.

Xu, L., Yang, X., Cui, S., Tang, J., Ding, S., Zhang, X. (2023). Co-occurrence of pluvial and fluvial floods exacerbates inundation and economic losses: evidence from a scenario-based analysis in Longyan, China. Geomatics, Natural Hazards and Risk, 14(1), 2218012.

Yang, Y., Sun, L., Li, R., Yu, D. 2020. Linking a Storm Water Management Model to a Novel Two-Dimensional Model for Urban Pluvial Flood Modeling. International Journal of Disaster Risk Science, 11, 508–518.

Zandsalimi, Z., Feizabadi, S., Yazdi, J., Neyshabouri, S.A.A.S. (2024). Evaluating the Impact of Digital Elevation Models on Urban Flood Modeling: A Comprehensive Analysis of Flood Inundation, Hazard Mapping, and Damage Estimation. Water Resources Management, 38, 4243–4268.

ZASTOSOWANIE MODELU HYDRAULICZNEGO 2D MIKE+ DO MODELOWANIA POWODZI RZECZNYCH I OPADOWYCH: STUDIUM PRZYPADKU NA SŁOWACJI

ABSTRAKT

Cel badania
Celem badania była symulacja zasięgu i głębokości powodzi rzecznych i opadowych w różnych scenariuszach przy użyciu dwuwymiarowego modelu hydraulicznego MIKE+ w połączeniu z systemami informacji geograficznej (GIS).

Materiały i metody
W przypadku powodzi rzecznych przyjęto warunki przepływu w stanie ustalonym dla trzech scenariuszy powodziowych (Q_{10}, Q_{100} i Q_{1000}). Modelowe mapy powodziowe zostały porównane z oficjalnymi mapami powodziowymi przygotowanymi w ramach drugiego cyklu Dyrektywy Powodziowej UE (2007). W odniesieniu do powodzi opadowych zastosowano metodę opadów na siatce, w której opady deszczu zostały ustalone dla trzech stałych intensywności (20, 40 i 60 mm/godz.) w dwóch scenariuszach: gleby w pełni nasycone i straty infiltracyjne. Obszarem badań był odcinek rzeki Teplica (3,68 km) w zachodniej Słowacji.

Wyniki i wnioski
Zgodnie z uzyskanymi wynikami różnica w zasięgu powodzi w stosunku do oficjalnych map powodziowych wyniosła odpowiednio: 0,009, 0,075 i 0,123 km^2 dla Q_{10}, Q_{100} i Q_{1000}. W przypadku scenariuszy opadów wynoszących 20, 40 i 60 mm/godz. oraz całkowicie nasyconych gleb, odpowiednio 13,5, 22,1 i 29,2% obszaru wykazywało głębokość przepływu między 0,005 a 0,1 m, podczas gdy 2,0, 4,2 i 6,1% obszaru wykazywało głębokość przepływu powyżej 0,1 m. W przypadku scenariuszy opadów wynoszących 20, 40 i 60 mm/godz. z uwzględnieniem strat infiltracyjnych, odpowiednio 6,0, 14,6 i 22,7% obszaru charakteryzowało się głębokością przepływu wynoszącą od 0,005 do 0,1 m, natomiast 0,4, 2,5 i 4,5% obszaru – głębokością przepływu powyżej 0,1 m. Po zastosowaniu współczynników infiltracji dla poszczególnych klas pokrycia terenu zasięg powodzi opadowej zmniejsza się odpowiednio o 58,2%, 34,4% i 23,2% dla scenariuszy opadów wynoszących 20, 40 i 60 mm/godz.

Słowa kluczowe: powódź rzeczna, powódź opadowa, modelowanie hydrauliczne, zagrożenie powodziowe, Słowacja